

February 29, 1988

TO: Magnet Division
FROM: Michael Chapman *MC*
SUBJECT: Calculation of the Radial Deflections of the Return-end Bonnet

Attached, you will find my report entitled "ANSYS Calculation of the Radial Deflections of the Return-end Bonnet."

It is noted that these results differ considerably with those obtained by Tom Nicol (FNAL), who performed a similar calculation (2/15/88). The discrepancy is due primarily to the fact that the bonnet modeled by Tom did not have the end-most notch present in the Brookhaven type bonnet that I modeled. It turns out that this notch has great importance to the deflection of the bonnet, and actually is the determining factor as to whether or not the deflections of the bonnet are important vis-a-vis the measurement instruments attached to the bonnet. I have spoken to Tom, and he has indicated that his information concerning the bonnet geometry was taken from an earlier preliminary drawing which is no longer relevant.

If you have any questions concerning this report, or would like particular details which I have not included, please contact me at (415) 486-6882 or CSA::CHAPMAN.

- cc:
- Distribution
- C.L. Goodzeit
- T. Nicol
- C. Peters
- B. Wands

ANSYS CALCULATION OF THE RADIAL DEFLECTIONS OF THE RETURN-END BONNET

Michael Chapman

Superconducting Super Collider/Central Design Group

February 19, 1988

The following is a finite element calculation of the radial deflections of the return-end bonnet (Brookhaven type) produced by forces transmitted from the coil to the end plate to the retainer and finally to the bonnet itself. (See Figure 1) These deflections are of interest because of their possible effect on measuring instruments attached to the end of the bonnet.

Bonnet Geometry

All dimensions for the return bonnet were obtained from BNL Drawing No. 22D2104A "Magnets, Dipole; SSC 16.6M, 4CM-LLN-003 COLL' COIL YOKE; Bonnet-Return."

Material Properties

The bonnet and skin material is AISI 304SST. The following material properties were used ($T = 4K^{\circ}$):

Young's modulus: $E = 30.5 \times 10^6$ psi

Poisson's ratio: $\nu = 0.279$

(From McHenry, HI, "The Properties of Austenitic Stainless Steel at Cryogenic Temperatures," in Austenitic Steels at Low Temperatures, Eds. Reed, R.P., Horiuchi, T., p 7)

Finite Element Model Formulation

The last 12 in. of the bonnet skin assembly is used for this model. The bonnet geometry is modeled according to the BNL drawing, except for the following conservative simplifications:

- radiused grooves are modeled as rectangular grooves
- stress relieving fillets are ignored

Due to its axisymmetrical nature, it is possible to model the bonnet using axisymmetrical 2-D solid elements. The ANSYS "STIF2" 2-D 6-node triangular solid element is used. The STIF2 triangular element is chosen in preference to the STIF42 rectangular element due to the complicated geometry of the bonnet.

The model is divided into four regions to allow different element densities for different regions of interest. (See Figure 2) Three iterations of the model are performed, each with a different element density.

Iteration		<u># Elements</u>	<u># Nodes</u>
	K	151	424
	L	378	956
	M	916	2129

Figure 3 shows the element mesh for iteration M at the bonnet end.

Applied Forces

The total load on the end plate has been previously calculated by others to be 15,000 lbs., in the outward axial direction. The end plate is entirely supported by the retainer, and it follows that the total axially-directed load experienced by the retainer is also 15,000 lbs.

It is not clear at this point whether the retainer is simply supported by the bonnet, whether the support is fixed, or whether the support is a combination of simple and fixed.

Two load scenarios are calculated here.

Load Case #1:

Simply Supported Retainer. The bonnet experiences only an outwardly directed axial force of 15,000 lbs. (2,387 lbs./radian). In this model, the load is applied as shown in Figure 4.

Load Case #2:

Partially Fixed Retainer. In addition to the axial load of Load Case #1, the retainer also transmits a moment to the bonnet equaling 3600 inlb — (573 inlb/radian), as indicated by F_1 and F_2 in Figure 5.

$$F_1 - F_2 = 2387 \text{ lb/rad}$$

$$(F_1 + F_2) \frac{l}{2} = 573 \text{ inlb/rad}$$

$$l = 0.12 \text{ in}$$

$$F_1 = 5968.5 \text{ lb/rad}$$

$$F_2 = 3581.5 \text{ lb/rad}$$

In both load cases, at the boundary condition, $y = 0$, the model is restrained from moving axially, and free to move radially.

Calculation

The three iterations mentioned above are solved for both loading conditions. Radial displacement (along inside edge) vs axial location are found for both loading conditions.

Results

Figure 6 shows the configuration of the displaced longitudinal section of iteration K under Load Case #1 (applied axial force). Figure 7 shows the same for Load Case #2 (applied axial force and moment). Figure 8 is a graph of radial displacement (UX) vs axial distance from end, for Load Cases #1 and #2, iteration K. Figures 9, 10 and 11 plot the same UX vs axial distance from end for only the last 1.5 in. of the bonnet, for iterations K, L, and M respectively. The consistency of the results for the three iterations ($\pm 5\%$) indicates that the element density was appropriate for these purposes. The subsequent calculations will use the results from iteration M.

The angular displacement of the inside of the bonnet at the point of interest 0 - 0.5 in. from end is equivalent to the slope of UX vs axial distance for the same region. For Load Case #1, the slope in this region is relatively constant and equal to:

$$= 0.75 \times 10^{-3} \text{ in./in.}$$

For Load Case #2, the slope is equal to

$$= 1.875 \times 10^{-3} \text{ in./in.}$$

A cantilever fixed to the inner bonnet end surface, and extending to the centerline of the bonnet (~ 5 in.) would therefore displace axially 3.75 mils for Load Case #1 and 9.38 mils for Load Case #2 relative to the point of applied load on the bonnet (i.e., axial elongation of the 16.6 m long skin not included).

Stress contours were plotted for axial, radial, and azimuthal normal stresses as well as for shear stress in the radial, axial plane. Stresses are found to be within the yield limits of the material with the notable exception of the axial stress at the point of applied load.

Comments

The bonnet geometry is taken from an available BNL drawing. Differences in bonnets from magnet to magnet should be noted. The return bonnet is modeled in these calculations.

The material properties used are slightly "stiffer" than commonly used room temperature values.

As apparent from the results of Load Case #1 and Load Case #2 (and as anticipated), the magnitude and nature of the applied loads is of critical significance to this problem. If the retainer is loose fitting in its seat, it can be approximated as simply supported by the bonnet. (See Figure 12) The deflection of the end plate will readily deflect the retainer, and the distorted retainer will then tend to contact the bonnet at one point only, along a line very close to parallel to the bonnet centerline. If this scenario is correct, then the modeling of Load Case #1 is appropriate.

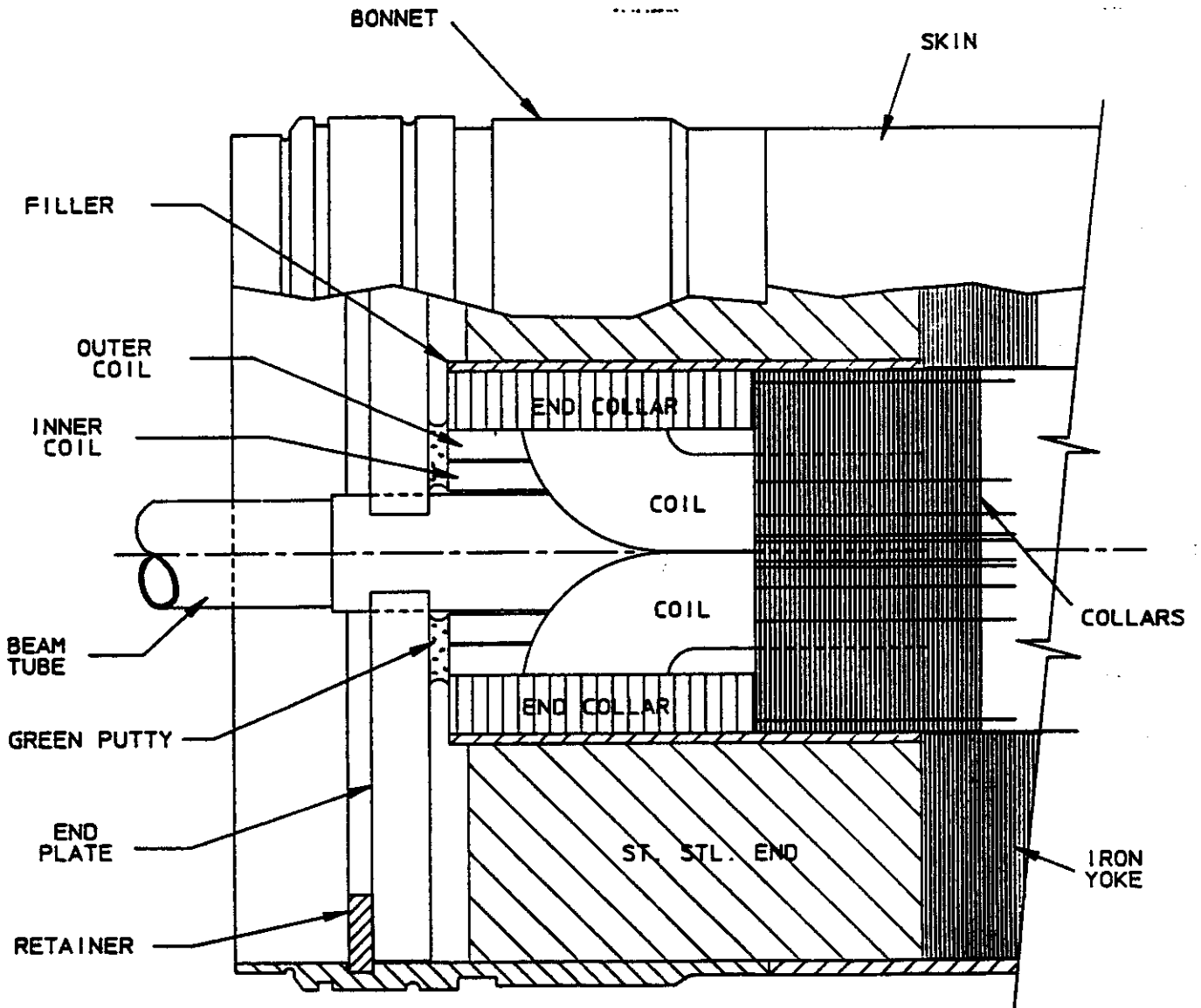
If, however, there is very little axial clearance between the retainer and the notch in the bonnet, as in Figure 13, the retainer is not simply supported but rather is fixed in some degree from rotating/pivoting with respect to the bonnet, and the exact loading of the bonnet becomes very difficult to determine and will be dependent on the degree to which the retainer is fixed and the angle of deflection of the end plate.

Because the degree that the retainer is fixed (if at all) and the angle of the deflection of the end plate is unknown, it is impossible to quantify the applied moment to the bonnet. It is possible to calculate its maximum, however, by assuming that the retainer is fully fixed and that the 15,000 lbs acts fully as a line load on the innermost edge of the retainer. The maximum calculated moment is 12,500 inlb or ~ 400% of that used in Load Case #2. Initially, this may seem like a high figure, but there is clearly at least some amount of "slop" in the retainer support and the applied load more accurately follows a distributed load rather than circular line load configuration. Both of these factors would greatly reduce the moment transmitted to the bonnet.

The moment applied to the bonnet in Load Case #2 is chosen rather arbitrarily, and the effects it has on the deflections of the bonnet are more illustrative than literal and show that if the retainer is fixed to any degree, that will have a significant effect on the results.

As was mentioned previously, the only excessive stress found is the axial stress at the point of loading. Whereas the forces were applied as point loads in our model, in actuality, they are probably distributed over a small region which would mitigate the high stress concentration at these points. It would be interesting, however, to field inspect these points for any yielding.

In summary, it seems evident that the radial deflections of the bonnet due to the loads transmitted from the coil are large enough to affect any measuring instruments affixed to its end. However, the exact magnitudes of these deflections are difficult to determine without knowing the exact support system of the retainer.

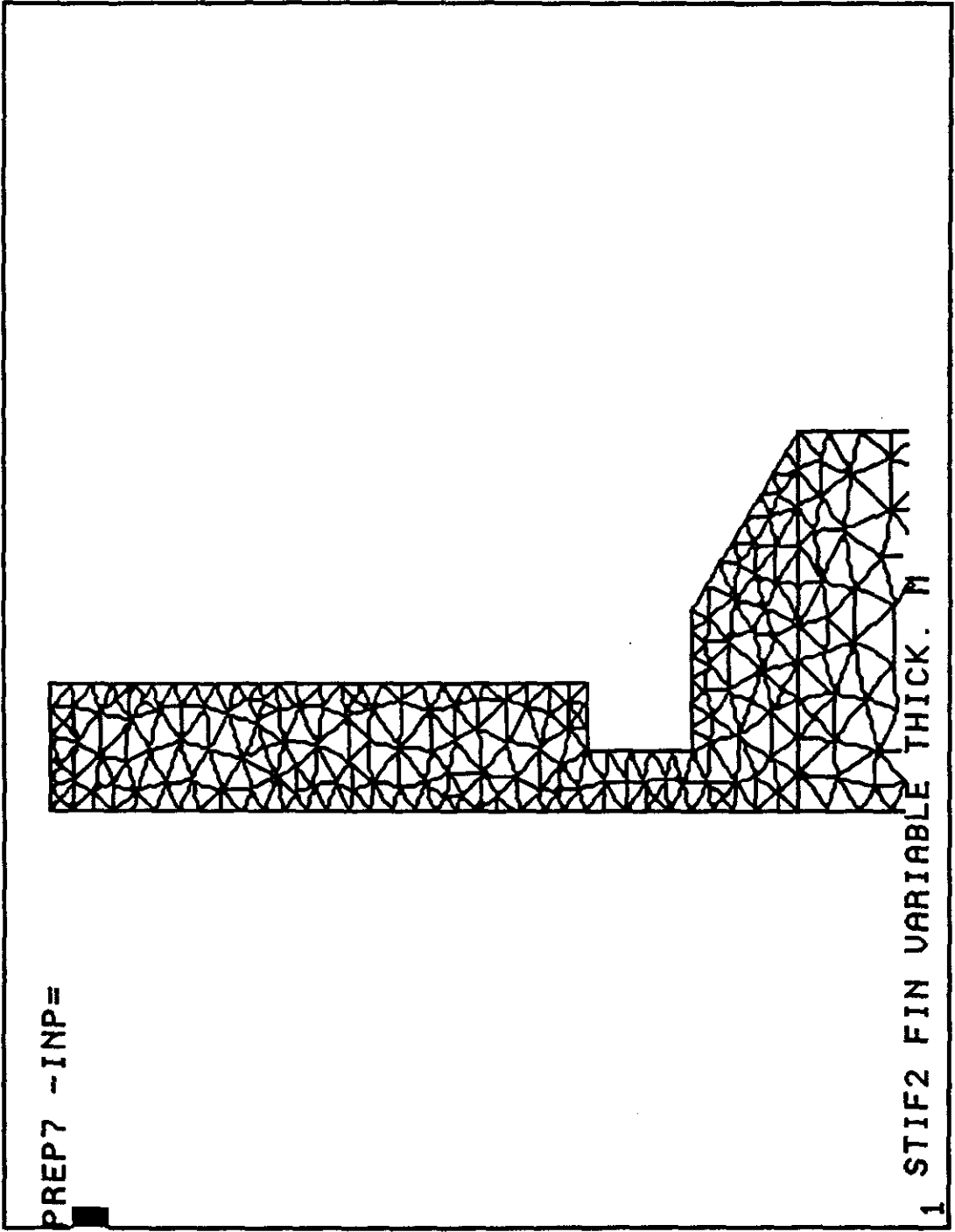


SECTION OF
END OF MAGNET

DISK: 34
RCOONRES MAG END SKETCH1
COONRES/CHAN 28 JAN 68

FIGURE 1

ANSYS 4.3
FEB 19 1988
10:50:34
PREP7 ELEMENTS
ZU=1
DIST= .55
XF=5.43
YF=11.5

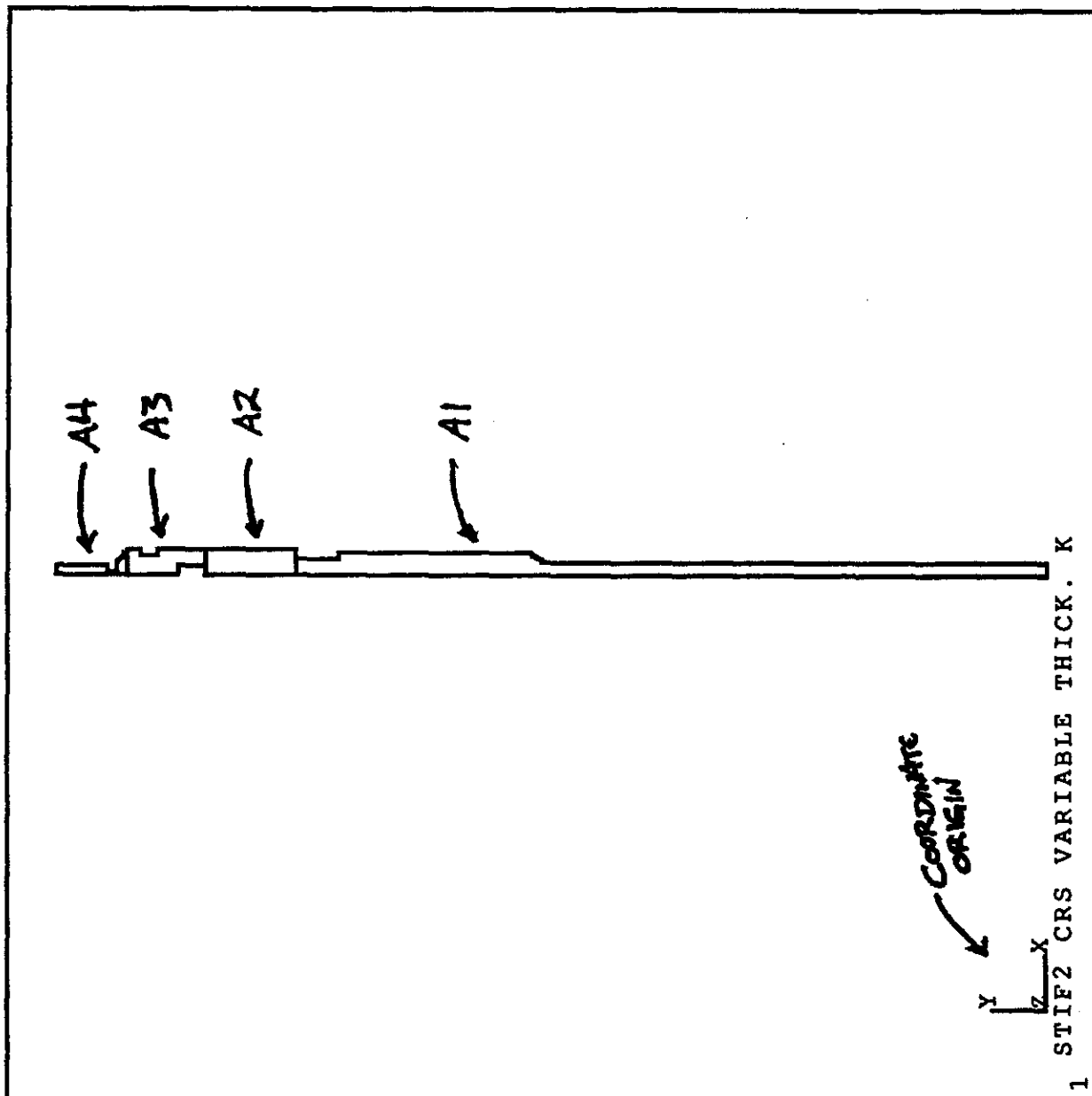


ELEMENT MESH FOR ITERATION M (DETAIL)
AT MODEL END

FIGURE 5

ANSYS 4.3
FEB 18 1988
17:03:38
PREP7 AREAS

ZV=1
DIST=6.6
XF=5.43
YF=6
EDGE

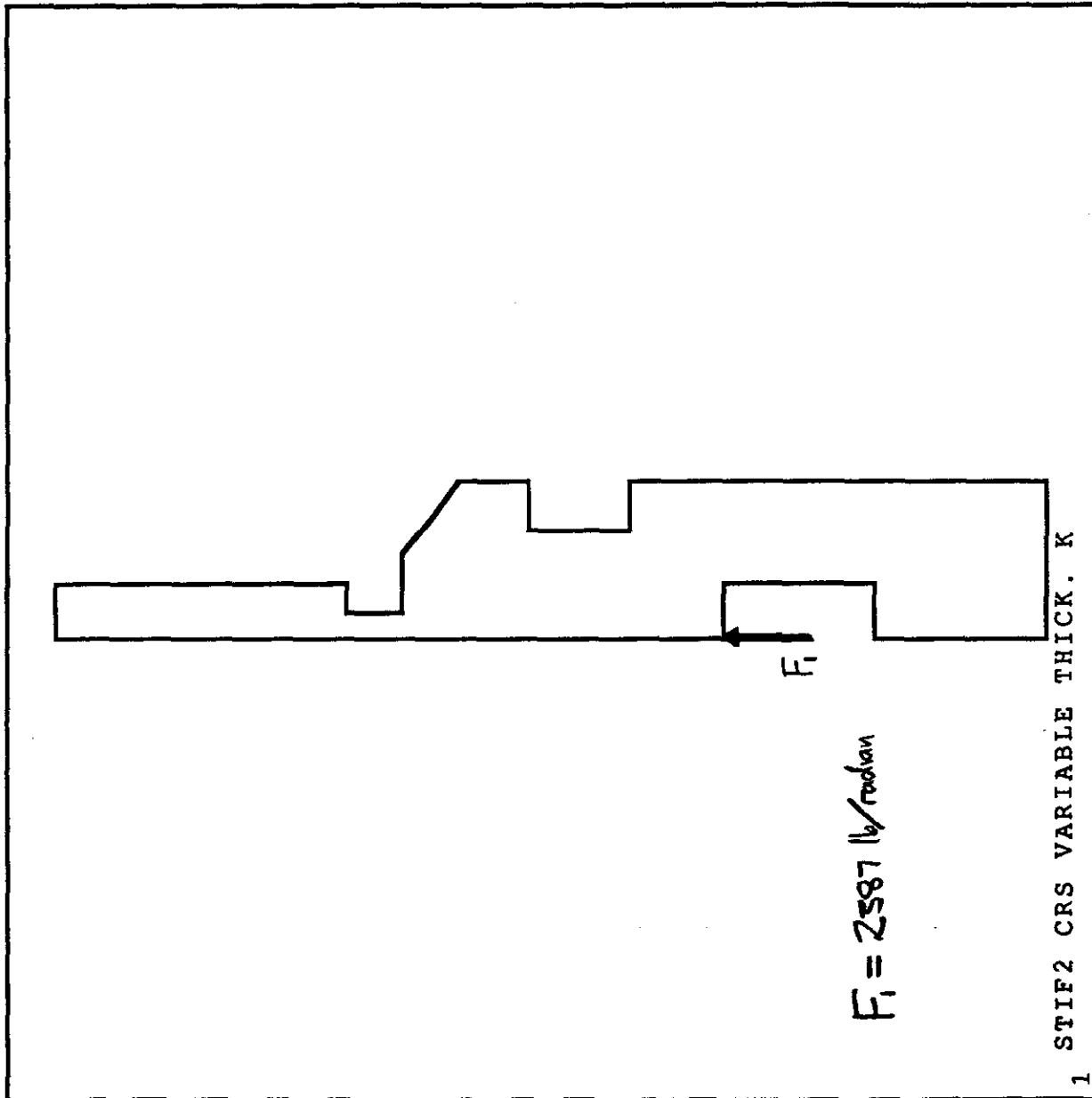


AXISYMMETRIC MODEL- DIVIDED INTO
4 REGIONS

Figure 2

ANSYS 4.3
FEB 18 1988
17:02:21
PREP7 ELEMENTS

ZV=1
DIST=1.17
XF=5.43
YF=10.9
EDGE

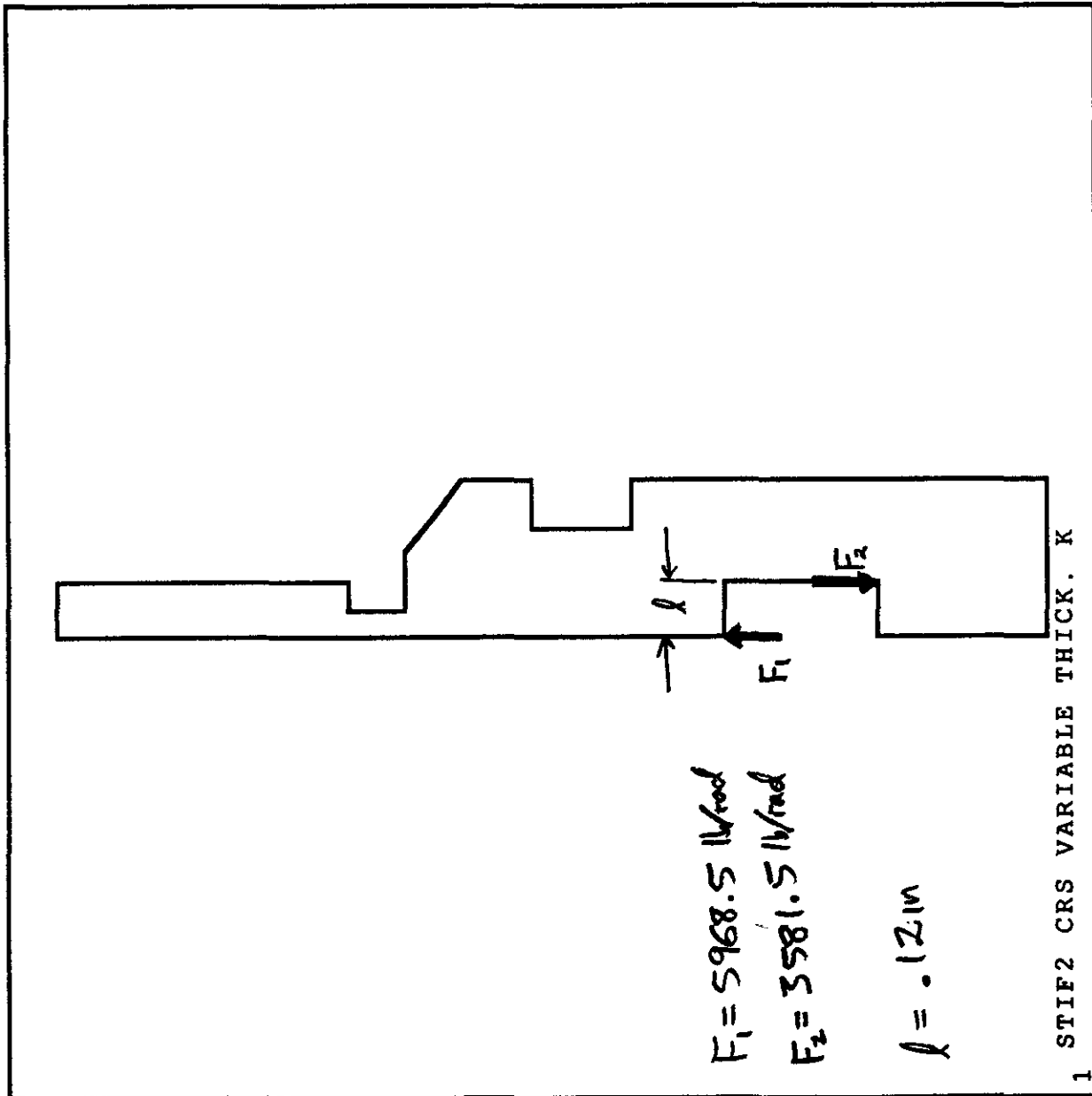


LOAD CASE #1

FIGURE 4

ANSYS 4.3
FEB 18 1988
17:02:21
PREP7 ELEMENTS

ZV=1
DIST=1.17
XF=5.43
YF=10.9
EDGE

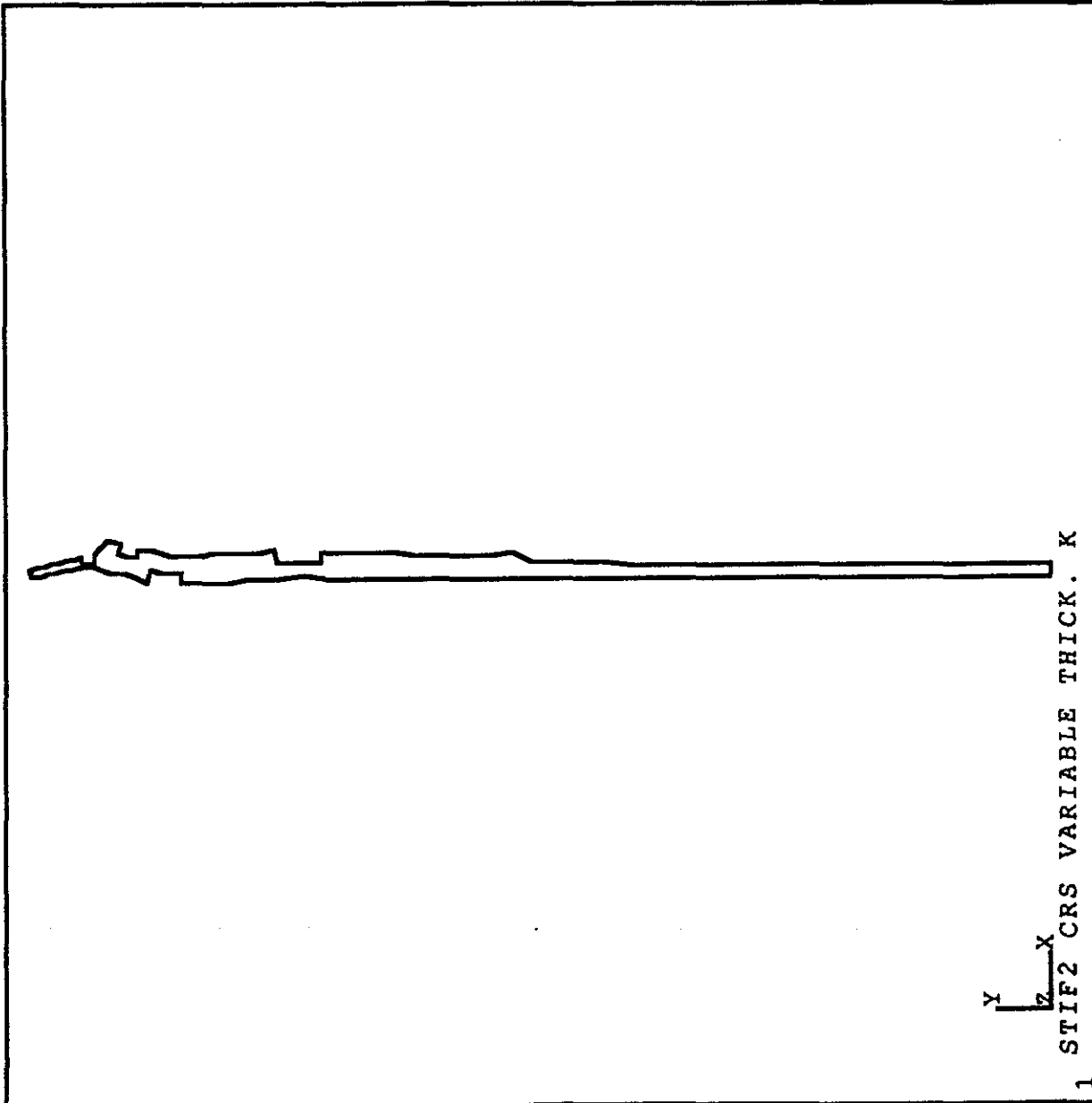


LOAD CASE #2

FIGURE 5

ANSYS 4.3
FEB 18 1988
17:08:18
POST1 DISPL.
STEP=1
ITER=1

ZV=1
DIST=6.6
XF=5.43
YF=6
EDGE
DMAX=.00108
* DSCA=300

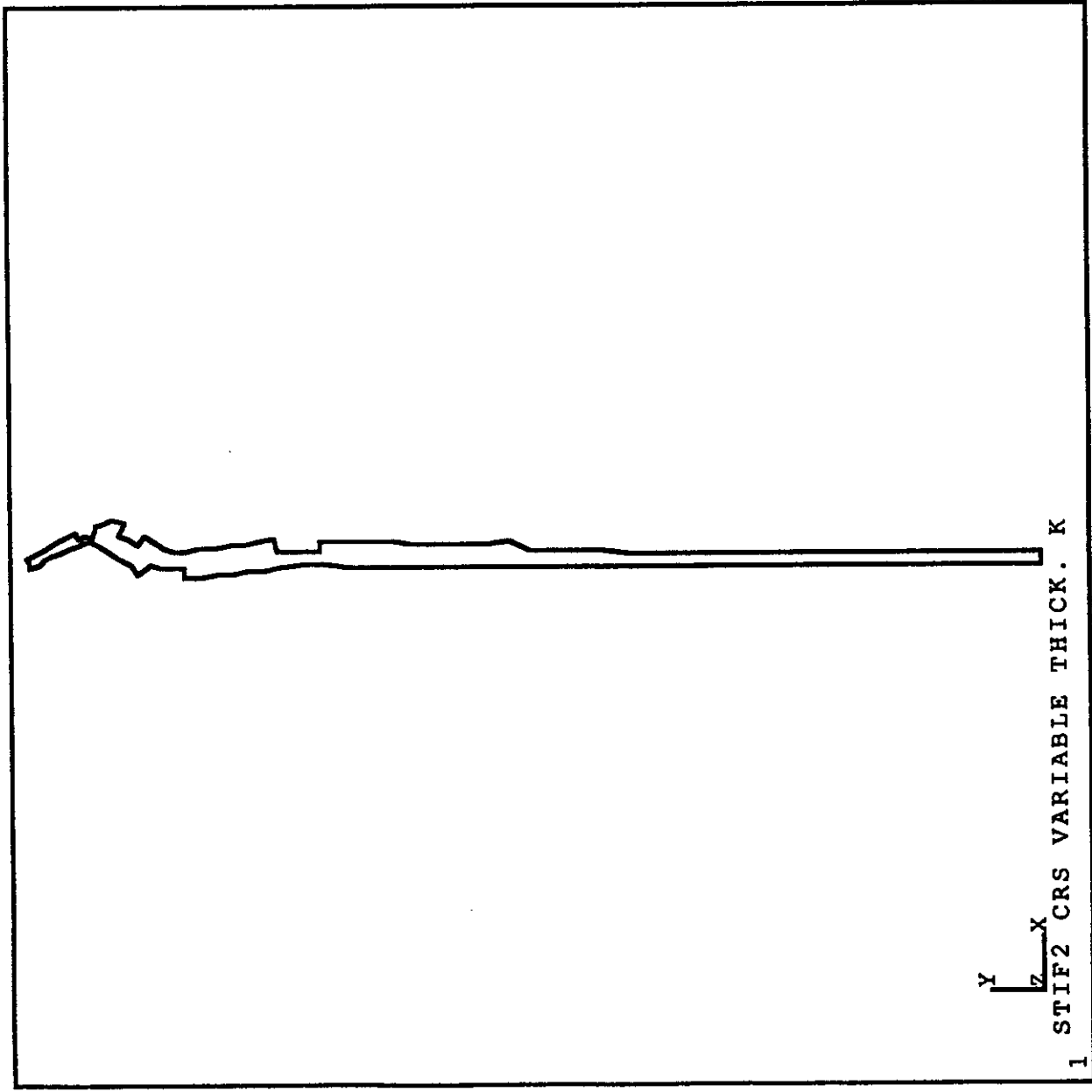


DISPLACEMENT CONFIGURATION UNDER
LOAD CASE #1

FIGURE 6

ANSYS 4.3
FEB 18 1988
17:07:52
POST1 DISPL.
STEP=2
ITER=1

ZV=1
DIST=6.6
XF=5.43
YF=6
EDGE
DMAX=.00166
* DSCA=300



DISPLACEMENT CONFIGURATION UNDER
LOAD CASE #2

Figure 7

ANSYS 4.3

FEB 18 1988

17:12:13

POST1

STEP=1

ITER=1

PATH PLOT

NOD1=363

NOD2=1

UX

DISPL NODAL

ZV=1

DIST=1.36

POST1

STEP=2

ITER=1

PATH PLOT

NOD1=363

NOD2=1

UX

DISPL NODAL

ZV=1

DIST=1.36

UX
(1E-3)

1.40

1.20

1.00

.80

.60

(1^m)

.40

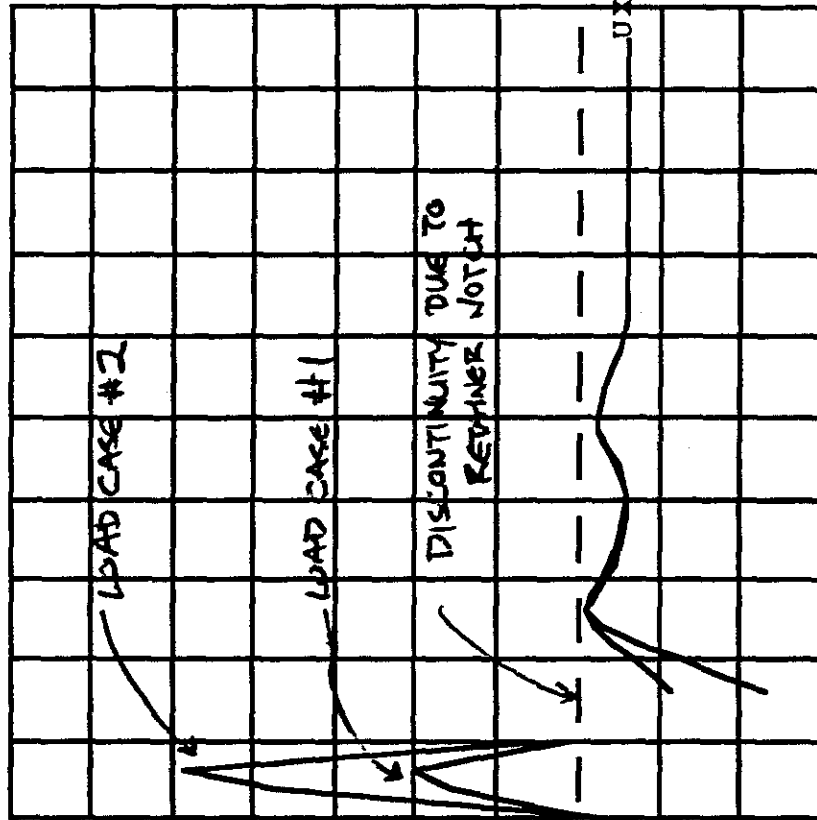
.20

0

-.20

-.40

-.60



DIST

12.5

11.3

10.0

8.8

7.5

6.3

5.0

3.8

2.5

1.3

DISTANCE FROM
BONNET END

1 STIF2 CRS VARIABLE THICK. K

FIGURE 8

ANSYS 4.3
 FEB 17 1988
 13:50:45

POST1
 STEP=2
 ITER=1
 PATH PLOT
 NOD1=363
 NOD2=273
 UX

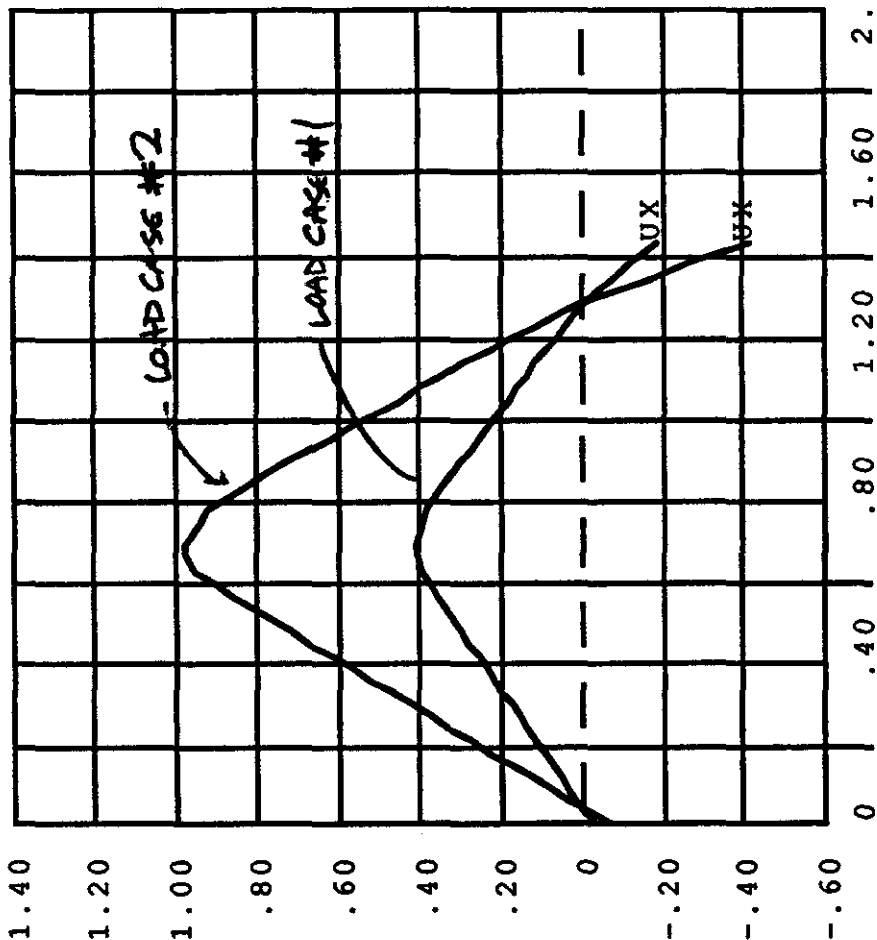
DISPL NODAL
 ZV=1
 DIST=1.36

POST1
 STEP=1
 ITER=1
 PATH PLOT
 NOD1=363
 NOD2=273
 UX

DISPL NODAL
 ZV=1
 DIST=1.36

FROM BONNET END

UX
 (1E-3)



1 STIF2 CRS VARIABLE THICK. K

RADIAL DISPLACEMENT VS. DIST. FROM END (UX vs. 12-Y)
 (ITERATION K)

FIGURE 9

ANSYS 4.3
 FEB 17 1988
 14:14:08

POST1
 STEP=2
 ITER=1
 PATH PLOT
 NOD1=787
 NOD2=539
 UX

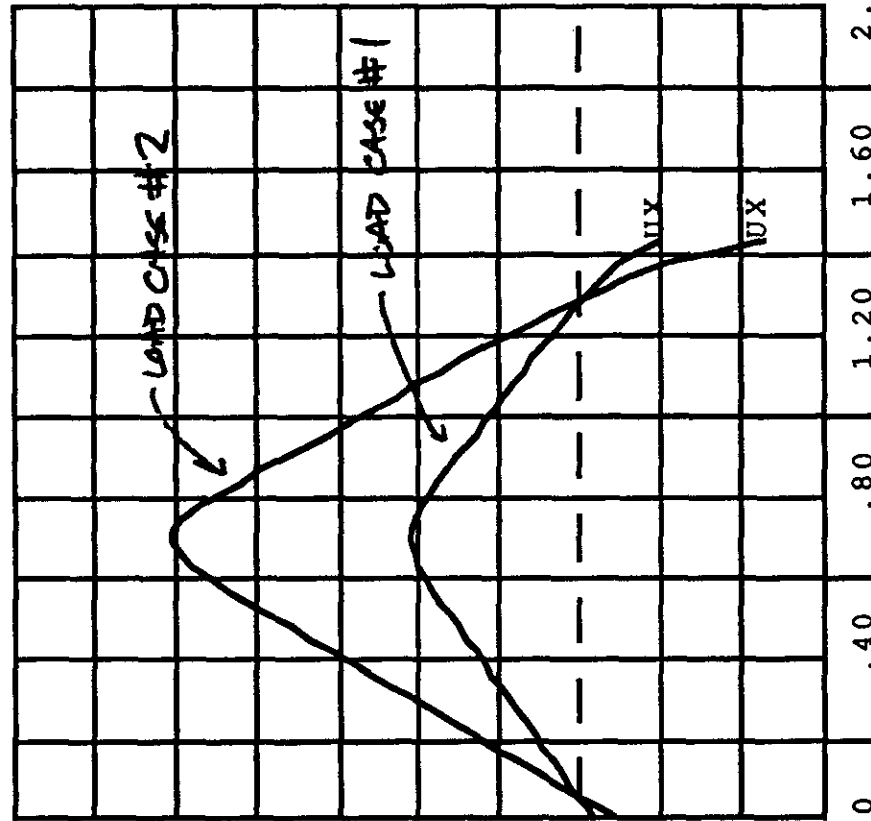
DISPL NODAL
 ZV=1
 DIST=1.36

POST1
 STEP=1
 ITER=1
 PATH PLOT
 NOD1=787
 NOD2=539
 UX

DISPL NODAL
 ZV=1
 DIST=1.36

FROM BUCKET END

UX
 (1E-3)



1 STIF2 MED VARIABLE THICK. L

RADIAL DISPLACEMENT VS. DIST. FROM END
 (ITERATION 1)

FIGURE 10

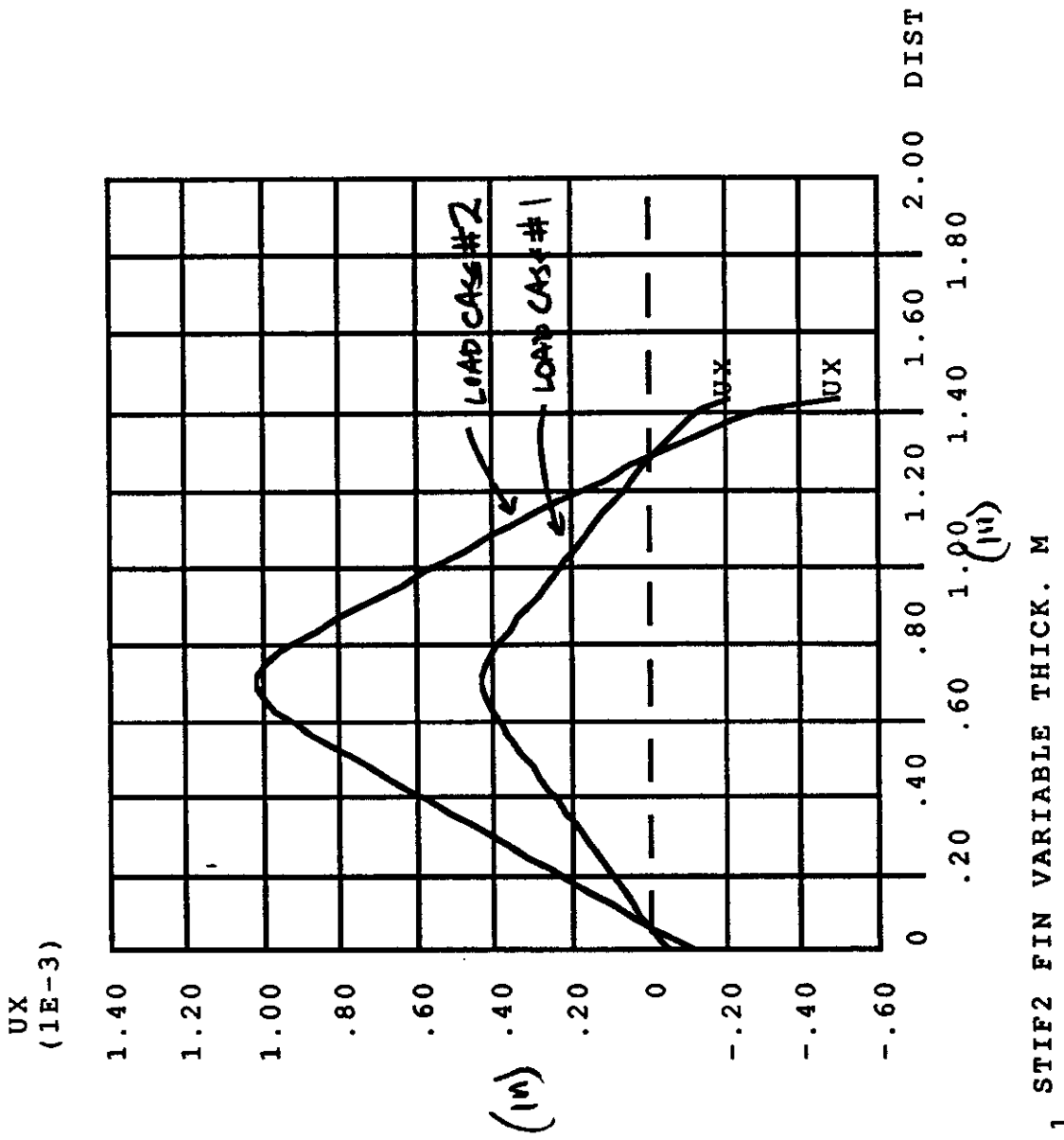
ANSYS 4.3
 FEB 17 1988
 14:48:46
 POST1

STEP=2
 ITER=1
 PATH PLOT
 NOD1=1508
 NOD2=779
 UX
 DISPL NODAL

ZV=1
 DIST=1.36

POST1
 STEP=1
 ITER=1
 PATH PLOT
 NOD1=1508
 NOD2=779
 UX
 DISPL NODAL

ZV=1
 DIST=1.36

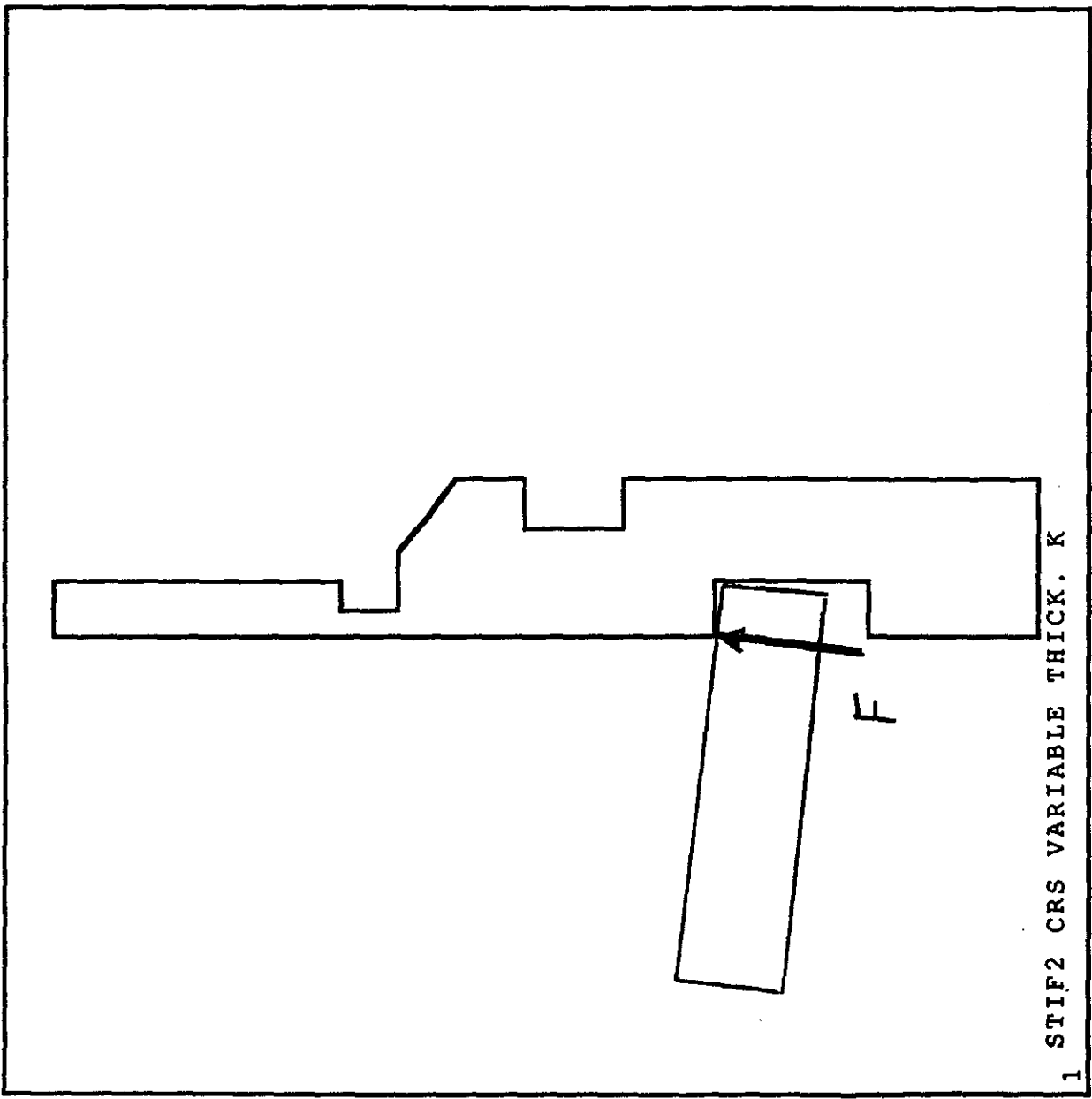


RADIAL DISPLACEMENT VS. DIST FROM END
 (ITERATION M)

Figure 11

ANSYS 4.3
FEB 18 1988
17:02:21
PREP7 ELEMENTS

ZV=1
DIST=1.17
XF=5.43
YF=10.9
EDGE



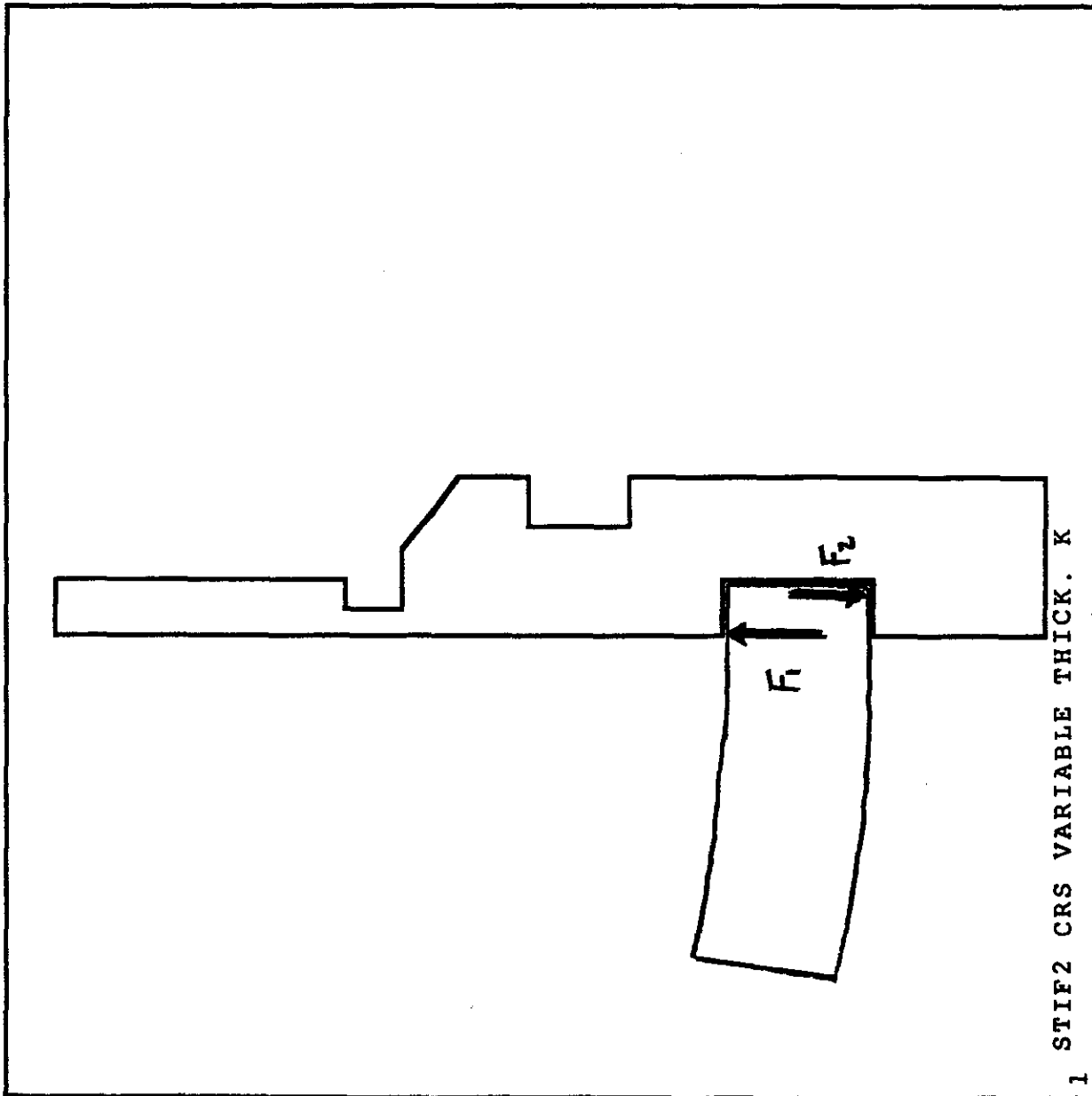
1 STIF2 CRS VARIABLE THICK. K

SIMPLY SUPPORTED RETAINER

FIGURE 12

ANSYS 4.3
FEB 18 1988
17:02:21
PREP7 ELEMENTS

ZV=1
DIST=1.17
XF=5.43
YF=10.9
EDGE



FIXED RETAINER

FIGURE 13